

## Local structural heterogeneities in liquid water under pressure

Murat Canpolat <sup>a,1</sup>, Francis W. Starr <sup>a</sup>, Antonio Scala <sup>a</sup>, M. Reza Sadr-Lahijany <sup>a</sup>,  
Osamu Mishima <sup>b</sup>, Shlomo Havlin <sup>a,c</sup>, H. Eugene Stanley <sup>a</sup>

<sup>a</sup> Center for Polymer Studies and Department of Physics, Boston University, Boston, MA 02215, USA

<sup>b</sup> National Institute for Research in Inorganic Materials (NIRIM), 1-1, Namiki, Tsukuba, Ibaraki 305, Japan

<sup>c</sup> Minerva Center and Department of Physics, Bar-Ilan University, Ramat-Gan, Israel

Received 5 May 1998; in final form 10 July 1998

### Abstract

We investigate the local structural heterogeneities that may appear in liquid water by studying a model of interacting water pentamers. We find local energy minima which we identify with well-defined configurations, and advance the hypothesis that one of these configurations may be related to local “high-density” structural heterogeneities occurring in liquid water when subjected to high pressure. Our results are consistent with experimental data on the effect of high pressure on the radial distribution function, and are further tested by molecular dynamics simulations reported here. © 1998 Published by Elsevier Science B.V. All rights reserved.

Walrafen pointed out that a wide range of experimental data are consistent with the possibility that each water molecule typically has four hydrogen bonds – giving rise to a pronounced peak in the oxygen–oxygen radial distribution function at about 2.8 Å, the nearest-neighbor distance [1–6]. Further, Walrafen noted that on time scales less than the lifetime of a hydrogen bond, he could identify a structural heterogeneity consisting of a water molecule and its four hydrogen bonded neighbors – a structure called the Walrafen pentamer. Using this pentamer as the basic unit, Walrafen described many features of the Raman spectra of water [1–6]. Ohtomo et al. showed that a combined analysis of X-ray and neutron diffraction data also suggests the presence of tetrahedral pentamer clusters [7]. More recently Kar-

maker and Joarder reproduced the radial distribution function of liquid water at room temperature using pentamers as the basic structural unit [8].

In this Letter, we investigate local structural heterogeneities in water by considering the interaction between pentamers, defined as a rigid structure composed of four water molecules located at the corners of a regular tetrahedron and hydrogen-bonded to a central molecule, with each O–O–O angle fixed at the tetrahedral value of 109.47°. The corner molecules are separated from the central molecule by 2.8 Å, corresponding to the first peak in the oxygen–oxygen radial distribution function  $g_{OO}(r)$  [9] <sup>2</sup>.

<sup>1</sup> Permanent Address: Department of Physics, Istanbul Technical University, Maslak, Istanbul 80626, Turkey.

<sup>2</sup> We present a definition of an ideal pentamer structure for the purposes of our model. In liquid water, one should allow reasonable flexibility in the bonding length and angle when identifying pentamer structures.

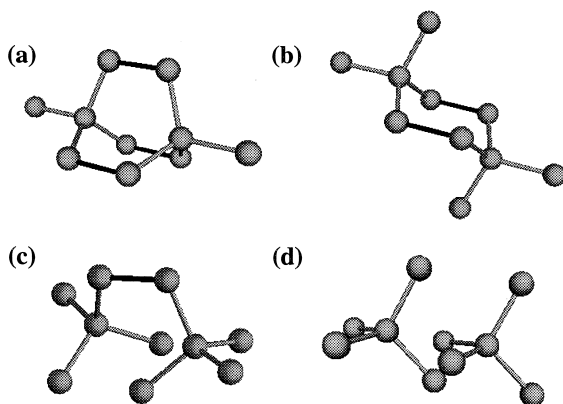


Fig. 1. Four local energy minima of two adjacent pentamers. The spheres represent water molecules, the solid tubes represent inter-pentamer hydrogen bonds, and the empty tubes denote intra-pentamer hydrogen bonds. (a) The three-bonded state; (b) the two-bonded state; (c) the one-bonded state; (d) zero hydrogen bonds between pentamers. Properties of each configuration are given in Table 1.

We consider two types of pentamer–pentamer interaction; a strong hydrogen bonding interaction between neighboring pentamers and a much weaker Lennard–Jones interaction between oxygens in different pentamers. Neighboring pentamers may be connected by three, two, one, hydrogen bonds or not connected by hydrogen bonds (Fig. 1). Configurations (a) and (b) in Fig. 1 are rigid and are local minima of the energy (because of the hydrogen bonds). We identify the most energetically favorable configurations with one and zero bonds (Fig. 1(c) and 1(d)), by minimizing the potential energy between two pentamers<sup>3</sup>, assuming that all non-hydrogen-bonded molecules of different pentamers  $\alpha$  and  $\beta$  have interactions much weaker than the hydrogen bond strength. We model the interactions that are not due to hydrogen bonding as

$$U_{\alpha\beta} = \sum_{i=0}^4 \sum_{j=0}^4 U_{\text{LJ}}(|\mathbf{r}_{\alpha i} - \mathbf{r}_{\beta j}|). \quad (1)$$

Here  $\mathbf{r}_{\alpha i}$  and  $\mathbf{r}_{\beta j}$  are the coordinates of the oxygens

<sup>3</sup> Using the relative orientation and separation of the two pentamers as degrees of freedom, we minimize the potential energy applying the Powell minimization routine; see Ref. [10].

of pentamers  $\alpha$  and  $\beta$ ; the oxygens interact by a Lennard–Jones potential  $U_{\text{LJ}}(r)$ . For the Lennard–Jones parameters  $\sigma$  and  $\epsilon$ , we use the values of the ST2 model of water<sup>4</sup>.

We notice that a liquid with a prevalence of configuration (d) will have a higher density than a liquid with an abundance of configurations (a), (b) or (c), since the distance between the pentamer centers is decreased in configuration (d) compared to the other configurations (column 3 of Table 1). Hence when pressure increases, we expect the number of non-hydrogen-bonded pentamers (high density structural heterogeneities of Fig. 1(d)) to increase and the number of bonded pentamers (low-density structural heterogeneities Fig. 1(a), (b)) to decrease.

The configurations with triply- and doubly-bonded pentamers (Fig. 1(a) and 1(b)) resemble the local structure of ice  $I_h$ <sup>5</sup>, while the configuration with non-hydrogen-bonded pentamers (Fig. 1(d)) is not unlike the local structure found in ice VI and ice VII, which are characterized by interpenetrating tetrahedra. It has been shown by MD simulations of water that under high pressure an interpenetrating network of hydrogen bonds forms, resembling ice VII structure [13,14], and that the distance between nearest neighbors does not change while the second-neighbor distance becomes smaller [13–18].

Experimental evidence for the possible existence of high-density structural heterogeneities similar to the structure of ice VI (and therefore consistent with the possible existence of high-density heterogeneities) has been found in high pressure measurements of the pair correlation function along paths such as that indicated in Fig. 2 [19,20]. We therefore carry out MD simulations of liquid water following the same path. We simulate three state points at pressures  $P = -2, 1$ , and 6 kbar and temperature 10 K above the temperature of maximum density

<sup>4</sup> For ST2,  $\epsilon = 316$  J/mol and  $\sigma = 3.1$  Å are the parameters for the Lennard–Jones potential  $U_{\text{LJ}} = 4\epsilon((\sigma/r)^{12} - (\sigma/r)^6)$ . See Ref. [11]. We have tuned  $\sigma$  and  $\epsilon$  over a range of values and find that the relative orientation of the pentamers does not change for each configuration.

<sup>5</sup> Configurations not unlike ice  $I_h$  have been previously predicted and observed in several studies. See Ref. [12] and references therein.

Table 1

Properties of each configuration shown in Fig. 1; here  $n(r)$  denotes the number of molecules separated by a distance  $r$ .

Configuration	Inter-pentamer bonds	Center-center separation (Å)	$n(2.8 \text{ Å})$	$n(4.5 \text{ Å})$	$n(3.4 \text{ Å})$
(a)	3	4.67	11	18	0
(b)	2	5.36	10	16	0
(c)	1	4.77	9	14	3
(d)	0	4.06	8	12	8

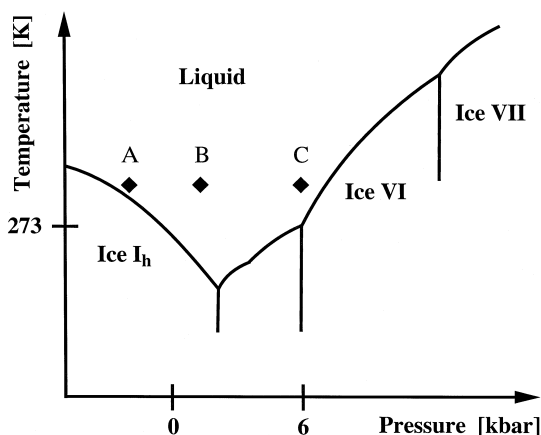


Fig. 2. Schematic of the phase diagram of water showing the simulated points between ice  $I_h$  and ice VI, corresponding to the path of previous experiments [19,20].

(TMD)<sup>6</sup>. We observe the same changes in  $g_{OO}(r)$  as seen experimentally: as pressure increases, an increase in the 3.4 Å (Fig. 3) peak and a decrease in the peaks at 2.8 Å and 4.5 Å occurs [19,20]. The distance 3.4 Å corresponds to the second neighbor distance in the configuration of Fig. 1(d) (Table 1). The decrease in the 2.8 Å and 4.5 Å peaks corresponds to the fact that the non-bonded configuration has two fewer 2.8 Å bonds and four fewer 4.5 Å next-nearest-neighbors (Table 1) compared to the lowest-density configuration of Fig. 1(b).

<sup>6</sup> We simulate 8000 water molecules interacting via the extended simple point charge model (SPC/E) [21]. We control temperature and pressure using the methods of Ref. [22]. Long range interactions are accounted for by the reaction-field technique with a cutoff at 7.9 Å [23]. Temperature is given relative to the TMD at atmospheric pressure, which is known to be approximately 245K for SPC/E (see Ref. [24–26]).

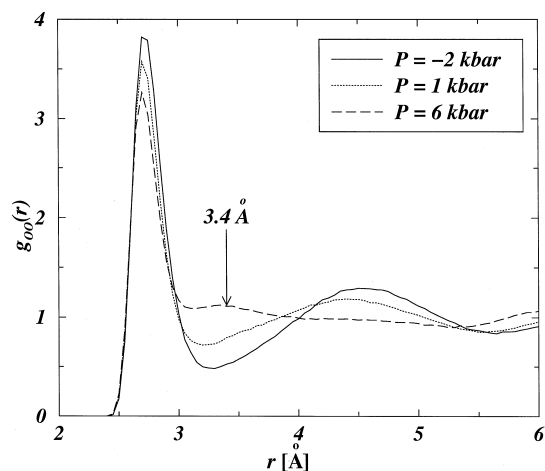


Fig. 3. The oxygen–oxygen radial distribution function for the three state points for which we carried out MD simulations. The temperature for the three state points simulated is 10 K above the TMD (see footnote 6). When pressure increases, the configuration of Fig. 1(d) is favored, as it has the smallest center-to-center separation (Table 1), so the value of  $g_{OO}(r)$  decreases for  $r \approx 2.8 \text{ Å}$  and  $r \approx 4.5 \text{ Å}$ , and increases for  $r \approx 3.4 \text{ Å}$  (consistent with the last three columns of Table 1).

It has been found that near a melting line, local structural heterogeneities are present in the liquid phase – with a typical diameter of a few atoms – in which the local order is not unlike the local order of the solid phase [27–29]<sup>7</sup>. Since  $H_2O$  has more than one crystalline phase; we expect then the local structure of the liquid to change upon pressure from resembling the low-density solid phase to resemble the high-density one.

In summary, we found that a highly simplified model of water based on water pentamers in a

<sup>7</sup> Locally-structured regions are shown in, e.g., Fig. 2 (a) of Ref. [30]. See also Ref. [31,32] and the review article in Ref. [33].

tetrahedral structure makes specific predictions about the local structural heterogeneities in water which resemble the structures of the low pressure ice  $I_h$  and high pressure ice VI or VII. The picture presented here may also help in understanding how a high pressure structure of interpenetrating tetrahedral sublattices can be formed in ice VI or VII <sup>8</sup>.

### Acknowledgements

We thank M.-C. Bellissent-Funel, P.G. Debenedetti, P.Ch. Ivanov, M. Meyer, P.H. Poole, P. Ray, S. Sastry, F. Sciortino, and G.E. Walrafen for enlightening discussions. Simulations were performed using the 192-processor SGI Origin 2000 supercomputer at the Boston University Center for Computational Science. MC is supported by the Scientific and Technical Research Council of Turkey, FWS by a NSF fellowship, and the Center for Polymer Studies by the NSF and British Petroleum.

### References

- [1] G.E. Walrafen, *J. Chem. Phys.* 40 (1964) 3249.
- [2] G.E. Walrafen, *J. Chem. Phys.* 47 (1967) 114.
- [3] W.B. Monosmith, G.E. Walrafen, *J. Chem. Phys.* 81 (1984) 669.
- [4] G.E. Walrafen, M.S. Hokmabadi, W.-H. Yang, *J. Chem. Phys.* 85 (1986) 6964.
- [5] G.E. Walrafen, M.R. Fisher, M.S. Hokmabadi, W.-H. Yang, *J. Chem. Phys.* 85 (1986) 6970.
- [6] G.E. Walrafen, W.-H. Yang, Y.C. Chu, M.S. Hokmabadi, *J. Chem. Phys.* 100 (1996) 1381.
- [7] N. Ohtomo, K. Tokiwano, K. Arakawa, *Bull. Chem. Soc. Jpn.* 54 (1981) 1802.
- [8] A.K. Karmakar, R.N. Joarder, *Phys. Rev. E* 47 (1993) 4215.
- [9] H.-D. Lüdemann, E.W. Lang, *Angew. Chem.* 21 (1982) 315.
- [10] W.H. Press, S.A. Teukolsky, W.T. Vetterling, B.P. Flannery, *Numerical Recipes* (Cambridge University Press, Cambridge, 1992).
- [11] F.H. Stillinger, A. Rahman, *J. Chem. Phys.* 60 (1974) 1545.
- [12] M.-C. Bellissent-Funel, J. Teixeira, L. Bosio, J.C. Dore, *J. Phys. Condensed Matter* 1 (1989) 7123.
- [13] F.H. Stillinger, A. Rahman, *J. Chem. Phys.* 61 (1974) 4973.
- [14] J.S. Tse, M.L. Klein, *J. Chem. Phys.* 92 (1987) 315.
- [15] R.W. Impey, M.L. Klein, I.R. McDonald, *J. Chem. Phys.* 74 (1981) 647.
- [16] J.D. Madura, B.M. Pettitt, *Mol. Phys.* 64 (1988) 325.
- [17] E. Shiratani, M. Sasai, *J. Chem. Phys.* 104 (1996) 7671.
- [18] E. Shiratani, M. Sasai, *J. Chem. Phys.* 108 (1998) 3264.
- [19] A.V. Okhulkov, Yu.N. Demianets, Yu.E. Gorbaty, *J. Chem. Phys.* 100 (1993) 1578.
- [20] M.-C. Bellissent-Funel, L. Bosio, *J. Chem. Phys.* 102 (1995) 3727.
- [21] H.J.C. Berendsen, J.R. Grigera, T.P. Stroatsma, *J. Phys. Chem.* 91 (1987) 6269.
- [22] H.J.C. Berendsen et al., *J. Chem. Phys.* 81 (1984) 3684.
- [23] O. Steinhauser, *Mol. Phys.* 45 (1982) 335.
- [24] L.A. Baez, P. Clancy, *J. Chem. Phys.* 101 (1994) 9837.
- [25] S. Harrington et al., *J. Chem. Phys.* 107 (1997) 7443.
- [26] K. Bagchi, S. Balasubramanian, M.L. Klein, *J. Chem. Phys.* 107 (1997) 8561.
- [27] F.H. Stillinger, T.A. Weber, *Phys. Rev. A* 25 (1982) 978.
- [28] K.J. Strandburg, *Rev. Mod. Phys.* 60 (1988) 161.
- [29] H.J.M. Hanley, T.R. Welberry, D.J. Evans, G.P. Morris, *Phys. Rev. A* 38 (1988) 1628.
- [30] M.A. Glaser, N.A. Clark, *Phys. Rev. A* 41 (1990) 4585.
- [31] M.A. Glaser, N.A. Clark, A.J. Armstrong, P.D. Beale, in: *Dynamics and Patterns in Complex Fluids*, edited by A. Onuki, K. Kawasaki (Springer-Verlag, Heidelberg, 1990), p. 141.
- [32] M.A. Glaser, N.A. Clark, in: *Geometry and Thermodynamics*, edited by J.-C. Tolédano (Plenum Press, New York, 1990), p. 193.
- [33] M.A. Glaser, N.A. Clark, *Adv. Chem. Phys.* 83 (1993) 543.
- [34] N.H. Fletcher, *The Chemical Physics of Ice* (Cambridge Univ. Press, Cambridge, 1970), p. 51.

<sup>8</sup> The crystalline phases of ice are shown in Ref. [34].